

**Design of a motion energy harvester based on compliant mechanisms
a bi-stable frequency up-converter generator**

Blad, T. W.A.; Farhadi Machekposhti, D.; Herder, J. L.; Tolou, N.

DOI

[10.1007/978-3-030-20131-9_160](https://doi.org/10.1007/978-3-030-20131-9_160)

Publication date

2019

Document Version

Final published version

Published in

Advances in Mechanisms and Machine Science

Citation (APA)

Blad, T. W. A., Farhadi Machekposhti, D., Herder, J. L., & Tolou, N. (2019). Design of a motion energy harvester based on compliant mechanisms: a bi-stable frequency up-converter generator. In T. Uhl (Ed.), *Advances in Mechanisms and Machine Science: Proceedings of the 15th IFToMM World Congress on Mechanism and Machine Science* (pp. 1619-1626). (Mechanisms and Machine Science; Vol. 73). Springer. https://doi.org/10.1007/978-3-030-20131-9_160

Important note

To cite this publication, please use the final published version (if applicable).
Please check the document version above.

Copyright

Other than for strictly personal use, it is not permitted to download, forward or distribute the text or part of it, without the consent of the author(s) and/or copyright holder(s), unless the work is under an open content license such as Creative Commons.

Takedown policy

Please contact us and provide details if you believe this document breaches copyrights.
We will remove access to the work immediately and investigate your claim.



Design of a Motion Energy Harvester based on Compliant Mechanisms: a Bi-stable Frequency Up-converter Generator.

T.W.A. Blad (t.w.a.blad@tudelft.nl) , D. Farhadi Machekposhti, J.L. Herder, and N. Tolou

Department of Precision and Microsystems Engineering, Delft university of technology, The Netherlands

Abstract. This work presents a novel design, model and prototype of a motion energy harvester based on bi-stability and frequency up-conversion. The Parametric Frequency up-converter Generator (PFupCG). The PFupCG was designed to harvest energy under conditions where the amplitude of the driving motion is larger than the internal displacement limit. Instead of an impact member, the PFupCG uses a compliant suspension mechanism that combines a bi-stable characteristic with a strong stiffening behavior as a result of geometric effects. This resulted in a prototype of the PFupCG with an internal-to-applied motion amplitude ratio of 0.2. A case study was carried out where the PFupCG was analyzed by simulation and experiment for vibration conditions representative of human walking motion (2 Hz, 25 mm).

Keywords: Motion energy harvesting, Frequency up-conversion, Bi-stability, Compliant mechanisms, Non-linear dynamics.

1 Introduction

Motion energy harvesting has been investigated for over 20 years since the early work of Williams and Yates in 1996 [1] which investigated the piezoelectric, electromagnetic, and electrostatic transduction mechanisms for the purpose of vibration-to-electric energy conversion. Devices incorporating such a transduction mechanism to generate electrical power from the energy of moving bodies are called motion energy harvesters (MEHs). MEHs have received much interest as they may provide a more sustainable alternative to batteries in powering low-power electronics such as wireless-sensor-networks. Moreover, one of the applications where MEHs could be applied is in the field of wearables, where energy can be harvested from human motion, analogue to the kinetic wristwatches.

General theoretical models for MEHs were constructed and analyzed thoroughly, which offered great insights in their performances under various operation conditions [2,3]. One of the main findings was that the highest efficiency is attained if the generator operates at resonance. Therefore, the natural frequency of the generator should be matched to the dominant frequency of the driving motion. These findings were further confirmed through simulations of those models with real human motion data [4] and a prototype attached to the upper arm [5].

However, although there is a wealth of energy available in human motion, is not a particularly convenient source of energy for the MEH. The frequencies are very low and the amplitudes of the motions are large w.r.t. the design space. For obvious reasons, the size of the MEH should not exceed the typical dimensions of the device it must power. The combination of the properties of human motion, the limited design space and the fact that only a finite amount of useful damping can be provided by the transducer has a devastating effect on the efficiency of MEHs that operate at resonance. Therefore, it becomes interesting to investigate other, more complex, dynamics and their efficiencies under these boundary conditions.

In recent years, great advances have been made towards this goal in prior art. Non-linear generators based on magnetic levitation have been developed and tested. An example is the device of Berdy et al. [6] which was tested on 10 subjects running 9.6 km h^{-1} and yielded an average output of $342 \mu\text{W}$. In Haroun et al. [7], a micro-electromagnetic MEH consists of a magnetic ball rolling through a tube wrapped by a coil was constructed. The power output was measured during three common activities at various locations on the body, and a maximum of $445 \mu\text{W}$ was observed. Also piezoelectric MEHs were developed such as the generator with a rotating proof mass demonstrated by Pillatsch et al. [8] and tested in a real world environment during a running race. It was shown that for frequencies from 0.5 – 4 Hz power outputs in the range of tens of micro watts were achieved. Another device was presented by Halim et al. [9] where the impact of a metal ball excited a PZT cantilever could generate up to $175 \mu\text{W}$ when excited by a vibration of 4.96 Hz with an acceleration of 2 g.

The research objective of this work is to present a new concept that uses bi-stability and frequency up-conversion to generate power from the unfavorable conditions of human motion. The scope features the mechanical design, a mathematical model, a prototype based on compliant mechanisms and an experiment.

Section II will present the mechanical design of the generator. In section III the mathematical model will be presented. The results of this experiment are presented in section IV and discussed in section V. Lastly, the conclusions will be summarized in section VI.

2 Mechanical design

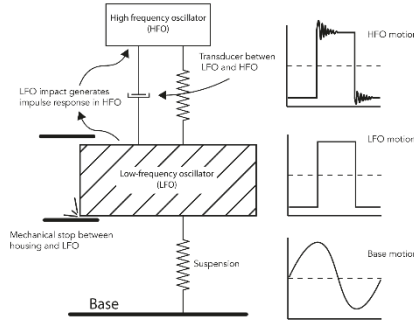


Fig. 1: Working principle of the parametric frequency up-converter generator (PFupCG).

To address the problem outlined in the previous section, the *Parametric Frequency up-Conversion Generator* (PFupCG), shown in Fig. 1, is proposed. The PFupCG is a non-resonant generator designed to harvest from vibrations with an amplitude larger than its internal displacement limit. We consider an harmonic driving motion with frequency ω and amplitude Y_0 to act on the base of the PFupCG. In the PFupCG the motion of an inertial mass, the low-frequency oscillator (LFO), is coupled to the motion of the base by a suspension. A compliant mechanism is proposed to increase the stiffness at the displacement limits and therefore act as a mechanical stop for the LFO. As a result, of the increased stiffness at the displacement limit, an impact-like behavior is exhibited between the LFO and the base. These impacts excite a secondary oscillator, the high-frequency oscillator (HFO), which is connected to the LFO by means of a spring and a transducer. Therefore, the HFO begins to vibrate at an increased frequency of $\omega_2 \gg \omega$. Electrical energy is generated in the transducer placed between the LFO and the HFO.



Fig. 2: Prototype of PFupCG.

Parameter	Symbol	Value
Motion amplitude ratio	MAR	0.2
Internal displacement limit	Z_l	5 mm
Total volume	V_t	614 cm ³
Total suspended mass	M_t	140 g
Suspension flexure length	L_s	35 mm
Suspension flexure width	b_s	10 mm
Suspension flexure thickness	h_s	0.05 mm
HFO mass	M_h	26 g
Intermediate body mass	M_i	33 g
HFO flexure lengths	L_i, L_h	20 mm
HFO flexure widths	b_i, b_h	10 mm
LFO-IB flexure thickness	h_i	0.20 mm
IB-HFO flexure thickness	h_h	0.10 mm
HFO natural frequency	ω_2	20 Hz

In order to maximize the output power, the energy in the impacts of the LFO should be maximized. This can be done by designing the suspension with a bi-stable characteristic [10] such that the LFO only moves if sufficient acceleration is applied. Based on this architecture, a prototype of the PFupCG was developed for energy harvesting from a target vibration with a frequency of 2 Hz and an amplitude of 25 mm, which is representative for human motion [11]. The internal displacement limit of the generator, Z_l , was selected to be 5 mm. This resulted in a device shown in Fig. 2 with an internal-to-applied Motion Amplitude Ratio (MAR) of 0.2 for the target operation conditions.

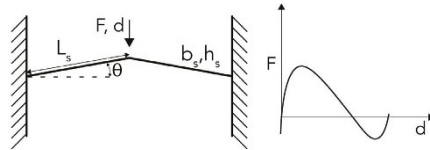


Fig. 3: Schematic representation of the bridge structure comprised of two flexures and sketch of force-deflection curve.

For the suspension of the PFupCG, a compliant mechanism is proposed which is comprised of eight spring steel ($E = 190$ GPa) flexure elements connected to the LFO body with mass M_l . The flexures are mounted in pairs at angles of $\theta = 10$ deg such that bridge structures are obtained, as shown in Fig. 3. These bridge structures allow motion through buckling of the flexures in one direction, but act as mechanical stops in the other direction because this loads the flexures in tension. In the prototype, two bridges facing upwards were combined with two bridges facing downwards. Consequently, pre-loading was induced by moving the end-points of the upwards and downwards facing bridges $2Z_l = 10$ mm apart and mounting the structure on a base. This procedure results in a bi-stable structure with stable positions at $z = Z_l$ and $z = -Z_l$. The result is a suspension mechanism that combines three functions of the PFupCG: 1) linear guiding of the LFO with, 2) a bi-stable characteristic and, 3) mechanical stops that facilitate impact behavior.

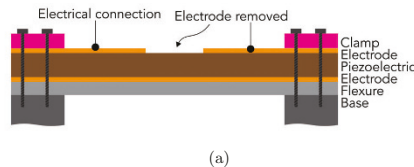


Fig. 4: Components of the piezoelectric transducer mounted between the intermediate body and the HFO.

The suspension of the HFO is also designed as a compliant mechanism which is comprised of four spring steel ($E = 190$ GPa) flexures, an intermediate body (IB) with mass M_i and the HFO body with mass M_h . The mechanism acts as a linear guiding and due to the intermediate body the parasitic rotations and translations are reduced. A piezoelectric transducer was placed on one of the flexures between the IB and the HFO. A sheet of PVDF from TE Connectivity (Part No. 3-1003702-7) with a thickness of $110 \mu\text{m}$ was attached on the topside of the flexure using epoxy (RS 553-614) and the middle part of the electrode on the top side of the PVDF was removed. The unimorph transducer was clamped using an insulating PLA clamp. A side view of the transducer assembly and its working principle is shown in Fig. 4.

The body parts of the PFupCG were manufactured from aluminum and resulted in a total suspended mass of $M_t = 140$ g. It was calculated that under the target excitation the prototype would undergo a maximum acceleration of $a = 4 \text{ m s}^{-2}$. Therefore, the bi-stable suspension must have break-away force smaller than 0.560 N. For the suspension of the HFO, the stiffness was designed such that the natural frequency of the HFO a factor 10 higher than the excitation frequency, $\omega_2 = 10\omega$. This resulted in the prototype shown in Fig. 2 with the mechanical parameters listed in the table next to the figure.

3 Mathematical model

An equivalent mechanical model is proposed for the PFupCG and is shown in Fig. 5. The bodies of the housing (i.e. the base), the LFO and the HFO are connected by nonlinear springs and dampers. The motions of the housing, the LFO and the HFO with respect to a fixed frame of reference are identified as $y(t)$, $x_1(t)$ and $x_2(t)$, respectively. Furthermore, the motions of the LFO and HFO relative to the base are $z_1 = x_1 - y$ and $z_2 = x_2 - y$. The LFO body has a mass of M_1 and is connected to the housing by the spring K_1 and damper C_1 . Additionally, the LFO is connected by the spring K_2 and damper C_2 to the body of the HFO, which has a mass of M_2 .

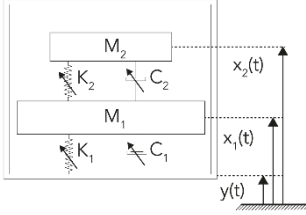


Fig. 5: Equivalent model of the system dynamics of the PFupCG

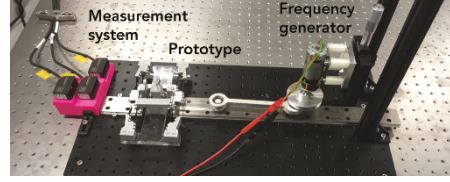


Fig. 6: Experimental setup consisting of crank-slider mechanism, laser position sensors and the PFupCG prototype.

In order to model the characteristics of the compliant suspension mechanism, a piecewise linear model with three stages is chosen for $K_1(z_1)$ and $C_1(z_1)$. The stages are respectively the negative stiffness region for $|z_1(t)| \leq Z_{1,1}$, a transition region for $Z_{1,1} < |z_1(t)| \leq Z_{1,2}$, and the mechanical stop region for $Z_{1,2} < z_1(t)$. In these regions the stiffnesses are $K_{1,1}$, $K_{1,2}$ and $K_{1,3}$ and the damping factors are $C_{1,1}$, $C_{1,2}$ and $C_{1,3}$, respectively. Therefore, a total of eight parameters are used to model the compliant suspension mechanism. For $K_2(z_2)$ and $C_2(z_2)$, which model the characteristics of the HFO, a piecewise linear model with two stages is used. Therefore, a total of five parameters are used for this spring-damper combination: $K_{2,1}$, $K_{2,2}$, $C_{2,1}$, $C_{2,2}$ and $Z_{2,1}$. The following equations of motion were found.

$$M_1 \dot{z}_1 + C_1(z_1) \dot{z}_1 + C_2(z_2) [\dot{z}_1 - \dot{z}_2] + K_1(z_1) z_1 + K_2(z_2) [z_1 - z_2] = -M_1 \ddot{y}. \quad (1)$$

$$M_2 \dot{z}_2 + C_2(z_2) [\dot{z}_2 - \dot{z}_1] + K_2(z_2) [z_2 - z_1] = -M_2 \ddot{y}. \quad (2)$$

The model was simulated using parameters given in Table. ?? and the PFupCG prototype was tested. The numerical result for the relative motion between the LFO and the HFO corresponds to the deflection of the piezoelectric element. Using a lumped-element approach, the electromechanical coupling of the transducer can be modeled [12,13]. Values of $C_p = 200$ pF and $R = 3.91$ M Ω were found by measuring the piezoelectric element and the resistor and a coupling factor of $\kappa = 35 \times 10^{-7}$ A m $^{-1}$ was found. The following differential equation was found to represent this circuit.

$$\dot{v}(t) = \frac{\kappa}{C_p} [z_2 - z_1] - \frac{v(t)}{RC_p} \quad (3)$$

In the experiment, the PFupCG prototype was driven by an electro-motor connected to a crank slider mechanism with a fixed amplitude of 25 mm. By controlling the voltage supplied to the electro-motor, the frequency of the driving motion could be varied. The motions of the base, $y(t)$, the LFO, $x_1(t)$ and the HFO, $x_2(t)$ are measured using laser distance sensors ILD 1420-200 from Micro-Epsilon, Ortenburg, Germany. Furthermore, the output voltage was measured over a 3.91 M Ω load using a multifunction I/O device NI USB-6211 from National Instruments. The experimental setup is shown in Fig. 6.

4 Results

The results of the numerical simulation are shown next to the experimental measurements in Fig. 7 and 8. Moreover, in these figures the output voltages and the relative displacements of the LFO are compared for excitation frequencies of 1 and 2 Hz, respectively. From the displacement measurements can be seen that impacts as a

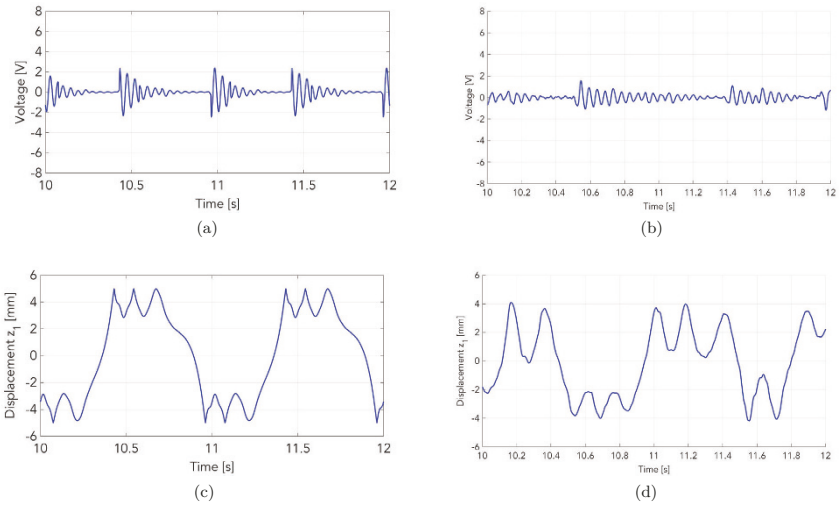


Fig. 7: Results of the numerical simulation (left) and experimental measurements (right) of the output voltage of the piezoelectric element (a-b) and the relative displacement of the LFO (c-d) for an input excitation with an amplitude of 25 mm and a frequency of 1 Hz.

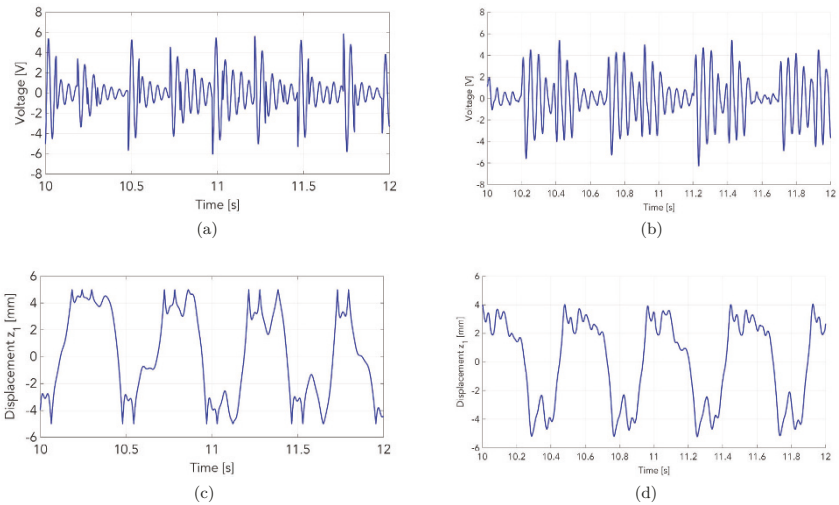


Fig. 8: Results of the numerical simulation (left) and experimental measurements (right) of the output voltage of the piezoelectric element (a-b) and the relative displacement of the LFO (c-d) for an input excitation with an amplitude of 25 mm and a frequency of 2 Hz.

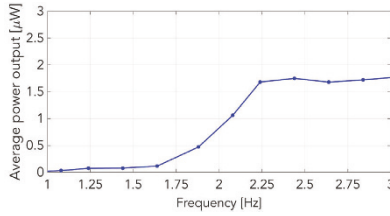


Fig. 9: Output power of the transducer for different operating frequencies.

result of the LFO engaging the mechanical stop mechanism occurs with a frequency of approximately twice the excitation frequency. It can be observed in the output voltage that these impacts trigger an impulse response in the HFO that is damped out over time. From the Fourier spectrum of the output voltage was found that most of the spectral content was located around a frequency of approximately 20 Hz, which corresponds to the lowest natural frequency of the HFO.

Comparing the displacement measurements for the excitation frequencies of 1 and 2 Hz it can be seen that the impacts occur with significantly higher velocity, and thus energy, in the latter case. It can be observed that the impact with higher energy results in a greater output voltage. The power output of the PFupCG is recorded over a range of frequencies between 1 and 3 Hz, while keeping the amplitude constant. The output power of the transducer is shown in Fig. 9 for different operating frequencies. The average power was found by the following formula.

$$P_{avg} = \frac{1}{R} \frac{1}{T} \int_{-\frac{T}{2}}^{\frac{T}{2}} V^2 dt \tag{4}$$

where the time interval T was taken as 20 seconds. In Fig. 9 the resulting power output is shown. It can be seen that for an excitation frequency below 1.6 Hz, virtually no output power is measured. Between 1.6 and 2.2 Hz it was found that the output power increased rapidly when the excitation frequency was increased up to a maximum of 1.8 µW. Further increasing the frequency beyond 2.2 Hz did not result in a higher power output.

5 Discussion

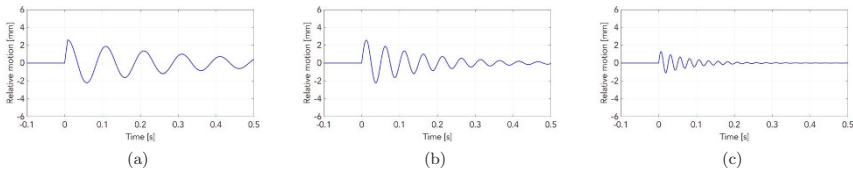


Fig. 10: Three cases of HFO motion for (a) UpF = 5, (b) UpF = 10 and (c) UpF = 20 subject to a displacement limit of 2.5 mm.

5.1 Up-conversion factor

In this work, an energy harvester concept was developed that aims to use the impact of an inertial mass (LFO) on a mechanical stop to excite a high-frequency harvesting element (HFO). In the PFupCG presented in this research, the natural frequency of the HFO was designed a factor 10 higher compared to the 2 Hz driving vibration. The up conversion factor, $UpF = \frac{\omega_2}{\omega}$ is an important design variable of frequency up-conversion systems and the following topics should be taken into consideration when selecting a value for the UpF. First

of all, the UpF should be large enough to constrain the HFO motion within the dimensions of the device to prevent impact between the LFO and the HFO and subsequently, loss of energy. However, the UpF should not be too large as this greatly limits the amplitude of the HFO motion, resulting in a lower relative velocity and thus lower power output. In general, it is advised that the UpF should be designed as such that the amplitude of the HFO motion is equal to the available space. This is depicted in Fig.10, where the responses of the HFO are simulated for three values of UpF subject to a 2.5 mm displacement limit. In this example, the highest output power was found for case b), where the HFO motion was kept precisely within the displacement limit.

5.2 Suspension model

The key modeling step in this research was the suspension model that governs the dynamics of the LFO around the displacement limit. In prior art where the mechanical stops are enforced by a collision member, a piecewise linear model with two stages was used. However, in this research the mechanical stop behavior results from a compliant suspension mechanism with a stiffening effect as a result of its geometry. Because the change in stiffness is much more gradual compared to a collision between bodies, this has to be taking into account in the equations of motion. Therefore, a piecewise linear model with three stages was proposed. In this model, a transition region was used to describe the characteristics of the compliant suspension mechanism more accurately.

In the experimental measurements of the LFO displacement in Fig. 7d and 8d the results of the transition regions on the dynamics can be observed. From the figures can be found that the shape of the LFO displacement is different when excited with 2 Hz compared to an excitation of 1 Hz. This is a result of the introduction of the transition region in the model and therefore this phenomenon is also found in the simulation results.

The most prominent difference between the simulation of the model and the experimental measurements is a slight preference of prototype for one of its stable positions. This result can be explained by manufacturing errors, or a slight offset of the setup from the horizontal such that gravity has a component in the DoF. This results in an asymmetric force-deflection graph which can in turn explain why the HFO of the experiment is more strongly excited when the LFO impacts the mechanical stop on the other side, and therefore show an irregular voltage response.

5.3 Frequency dependency

From Fig. 9 three regimes were identified with different relations between the excitation frequency and the output power. The PFupCG operates in the first regime for excitation frequencies up to 1.6 Hz. In this regime, the LFO may move between its two stable positions, but does not have enough energy to progress far into the transition area. As a result, the LFO impact is very light and the amplitude of the HFO motion is very small. Therefore, the power output is low. In the next regime, which occurs for excitation frequencies between 1.6 and 2.2 Hz it was found that the output power increased rapidly when the excitation frequency was increased. Here, enough power is supplied to the LFO to cross the transition region which results in a strong impact. Increasing the excitation frequency increases the energy of the impact which in turn increases the amplitude of the HFO motion, and therefore the power output. At an excitation frequency of 2.2 Hz, the impact energy is high enough to have the HFO motion reach its displacement limit, and impact on the LFO. As a result, the power output no longer increases beyond this frequency.

5.4 Performance and miniaturization of the PFupCG

A maximum power output of 1.8 μ W was measured over a frequency range of 2.2 – 3.1 Hz. This extremely low value is mainly due to the large dimensions of the prototype and the poor efficiency of the transducer. The transducer in this prototype was merely a qualitative demonstrator and the performance of the PFupCG could be improved by orders of magnitude by designing a proper transducer. Specifically, improvements such as using another piezoelectric material with a much higher coupling factor, such as PZT-5H, and manufacturing the transducer as a bi-morph can result in an increased power output.

6 Conclusion

The main contributions from this work are a new motion energy harvester concept based on bi-stability and frequency up-conversion, corresponding mathematical model and prototype. The Parametric Frequency up-converter Generator (PFupCG) is based on compliant mechanisms and has a strong stiffening effects at the desired displacement limits. For operating conditions where the driving motion has a larger amplitude than the

internal displacement limit of the generator, such as when harvesting from (low-frequency) human motion, the frequency up-conversion strategy can result in an increased power output. This was demonstrated by means of a simulation for a driving vibration with a frequency of 2 Hz and an amplitude of 25 mm using a generator with an internal-to-applied motion amplitude ratio of 0.2. Moreover, the PFupCG prototype validated the dynamical properties of model, but was unable to achieve a relevant power output as a result of its size and inefficient transducer design. It is expected that a miniaturized version of the PFupCG with a proper transducer can result in a competitive power output w.r.t. the state-of-the-art for the given conditions.

References

1. CB Williams and Rob B Yates. Analysis of a micro-electric generator for microsystems. *sensors and actuators A: Physical*, 52(1):8–11, 1996.
2. Paul D Mitcheson, Tim C Green, Eric M Yeatman, and Andrew S Holmes. Architectures for vibration-driven micropower generators. *Journal of microelectromechanical systems*, 13(3):429–440, 2004.
3. Paul D Mitcheson, Eric M Yeatman, G Kondala Rao, Andrew S Holmes, and Tim C Green. Energy harvesting from human and machine motion for wireless electronic devices. *Proceedings of the IEEE*, 96(9):1457–1486, 2008.
4. Thomas Von Buren, Paul D Mitcheson, Tim C Green, Eric M Yeatman, Andrew S Holmes, and Gerhard Troster. Optimization of inertial micropower generators for human walking motion. *IEEE Sensors Journal*, 6(1):28–38, 2006.
5. Matthias Geisler, Sebastien Boisseau, Matthias PEREZ, Pierre Gasnier, Jerome Willemin, Imene Ait-Ali, and Simon Perraud. Human-motion energy harvester for autonomous body area sensors. *Smart Materials and Structures*, 2016.
6. DF Berdy, DJ Valentino, and D Peroulis. Kinetic energy harvesting from human walking and running using a magnetic levitation energy harvester. *Sensors and Actuators A: Physical*, 222:262–271, 2015.
7. A Haroun, I Yamada, and S Warisawa. Investigation of kinetic energy harvesting from human body motion activities using free-impact based micro electromagnetic generator. *Diabetes Cholest metabol*, 1(104):13–16, 2016.
8. Pit Pillatsch, Eric M Yeatman, and Andrew S Holmes. A piezoelectric frequency up-converting energy harvester with rotating proof mass for human body applications. *Sensors and Actuators A: Physical*, 206:178–185, 2014.
9. Miah Abdul Halim and Jae Yeong Park. Piezoelectric energy harvester using impact-driven flexible side-walls for human-limb motion. *Microsystem Technologies*, pages 1–9, 2017.
10. Sergio P Pellegrini, Nima Tolou, Mark Schenk, and Just L Herder. Bistable vibration energy harvesters: a review. *Journal of Intelligent Material Systems and Structures*, page 1045389X12444940, 2012.
11. TWA Blad, D Farhadi Macheqposhti, JL Herdser, AS Holmes, and N Tolou. Vibration energy harvesting from multi-directional motion sources. In *2018 International Conference on Manipulation, Automation and Robotics at Small Scales (MARSS)*, pages 1–9. IEEE, 2018.
12. Yaowen Yang and Lihua Tang. Equivalent circuit modeling of piezoelectric energy harvesters. *Journal of Intelligent Material Systems and Structures*, 20(18):2223–2235, 2009.
13. Waleed Al-Ashtari, Matthias Hunstig, Tobias Hemsel, and Walter Sextro. Analytical determination of characteristic frequencies and equivalent circuit parameters of a piezoelectric bimorph. *Journal of Intelligent Material Systems and Structures*, 23(1):15–23, 2012.